

Available online at www.sciencedirect.com

SCIENCE @ DIRECT®

International Journal of Multiphase Flow 31 (2005) 824–842

International Journal of
Multiphase
Flow

www.elsevier.com/locate/ijmulflow

Experimental study of single bubble motion in a liquid metal column exposed to a DC magnetic field

C. Zhang, S. Eckert *, G. Gerbeth

MHD Department, Forschungszentrum Rossendorf, P.O. Box 510119, 01314 Dresden, Germany

Received 23 September 2004; received in revised form 4 May 2005

Abstract

The motion of single Argon bubbles rising in the eutectic alloy GaInSn under the influence of a DC longitudinal magnetic field (parallel to the direction of bubble motion) was examined. The magnetic field strength was varied up to 0.3 T corresponding to a magnetic interaction parameter N (which measures the ratio of electromagnetic forces to inertial forces) slightly greater than 1. The liquid metal was at rest in a cylindrical container. Bubble and liquid velocities were measured using ultrasound Doppler velocimetry (UDV). The measured bubble terminal velocity showed oscillations indicating a zigzag movement of ellipsoidal bubbles. For small bubbles ($d_e \leq 4.6$ mm) an increase of the drag coefficient with increasing magnetic interaction parameter N was observed, whereas for larger bubbles ($d_e \geq 5.4$ mm) the application of the magnetic field reduces the drag coefficient. The measurements revealed a distinct electromagnetic damping of the bubble induced liquid velocity leading to more rectilinear bubble trajectories when the magnetic field is applied. Moreover, significant modifications of the bubble wake structure were observed. Raising of the magnetic field strength caused an enlargement of the eddies in the wake. The Strouhal number decreases with increasing magnetic interaction parameter N .

© 2005 Elsevier Ltd. All rights reserved.

Keywords: Single bubble; Liquid metal; Magnetic field; Terminal velocity; Drag coefficient; Bubble wake; Ultrasound Doppler velocimetry

* Corresponding author. Tel.: +49 351 260 2168; fax: +49 351 260 2007.

E-mail address: s.eckert@fz-rossendorf.de (S. Eckert).

1. Introduction

Bubble driven flows have found wide applications in industrial technologies. In metallurgical processes gas bubbles are injected into a bulk liquid metal to drive the liquid into motion, to homogenise the physical and chemical properties of the melt or to refine the melt. For such gas–liquid metal two-phase flows, external magnetic fields provide a possibility to control the bubble motion in a contactless way.

Numerous experimental and theoretical studies have been carried out on the movement of bubbles in transparent liquids, especially in water. An air bubble keeps its spherical shape and rises rectilinearly in water, as long as the bubble diameter is less than 0.7 mm (Saffman, 1956). The behaviour of larger, ellipsoidal bubbles is unstable and shows a transition to non-rectilinear motion with zigzag or spiral trajectories. This phenomenon has mainly been attributed to the influence of the bubble wake. For a detailed review about the onset of bubble path instabilities we refer to Fan and Tsushiya (1990) or Magnaudet and Eames (2000). Ellingsen and Risso (2001) investigated 2.5 mm diameter air bubbles rising in water by high-speed video and LDA. They found path oscillations developed in the absence of shape oscillations. Two unstable modes were identified having the same frequency but showing a phase shift of $\pi/2$. The first appearing primary mode leads to a plane zigzag trajectory, whereas the secondary mode is shown to be responsible for the helical motion. The vertical velocity component was found to oscillate with twice the frequency of the horizontal ones, but with a weaker amplitude. Using dye visualisation Lunde and Perkins (1997) observed a continuous pair of parallel helical vortex filaments in the wake of a bubble rising on a spiral trajectory, while intermittent and alternately shed hairpin vortices were found behind a bubble moving on a zigzag path. Similar vortex structures have also been found by DPIV measurements behind bubbles with diameters from 4 to 8 mm (Brücker, 1999). Recently, de Vries et al. (2002) visualised bubble wakes by a Schlieren optics technique showing a double-threaded wake of zigzagging bubbles. The authors estimated the lift force induced by this wake structure on the bubble concluding that the zigzag motion may occur without periodic vortex shedding.

Our interest is devoted to the motion of gas bubbles in liquid metals under the influence of a DC magnetic field. Previous experimental work showed the effect of transverse and longitudinal magnetic fields, respectively, on the slip ratio and the bubble dispersion in a turbulent bubbly channel flow (Eckert et al., 2000a,b). In this paper, we consider the case of a single, isolated bubble rising in a cylindrical column of stagnant liquid metal exposed to a longitudinal magnetic field. Because the gas bubble is electrically non-conducting, it does not experience the effect of the electromagnetic force directly. However, the bubble behaviour can be expected to be influenced by the magnetically induced modifications in the liquid flow structure around the bubble. The possibility to influence the bubble wake by an additional body force may also contribute to a better general understanding of the interaction between bubble path and wake.

The number of publications dealing with gas bubbles rising in liquid metals is comparatively small. Andreini et al. (1977) detected the noise generated by the bubbles releasing from the orifice by means of an acoustic microphone attached to a brass seal. In this way the authors were able to determine the bubble formation frequency in tin and lead and consequently the equivalent bubble diameter. Schwerdtfeger (1968) used an ultrasonic pulse-echo instrument to study the rise of argon bubbles in mercury. The terminal velocities he determined in mercury were slightly smaller

than corresponding measurements in water. His data fit well with the theoretical expression derived by Mendelson (1967). Mori et al. (1977) studied the influence of a transverse magnetic field on the rise velocity of nitrogen bubbles in mercury. It was found that the magnetic field effect depends on the bubble size. Small bubbles with diameters of about 2 mm show a distinct helical motion without magnetic field. Here, the application of magnetic field intensities up to 1 T once increases the bubble velocity, before it decreases with a further increase of the field strength. For larger bubbles the terminal velocity decreases monotonically with increasing strength of the transverse field.

The shortage of suitable measuring techniques might be considered as a main reason for the relatively slow progress in the investigations of gas–liquid metal flows. Powerful optical methods as used for measurements in transparent liquids are obviously not available for applications in liquid metals. The majority of measurements in liquid metal two-phase flows published until now were obtained using local conductivity probes (e.g. Mori et al., 1977; Iguchi et al., 1997; Eckert et al., 2000a), hot wire anemometer (Toral, 1981) or optical fibre probes (Cartellier and Barrau, 1998) to determine quantities such as void fraction, bubble and liquid velocity or the bubble size. However, measurements with any local probe disturb the flow in a significant way, especially if the structures to be investigated reach dimensions comparable to the probes. Diversions of bubble trajectories can be observed in the vicinity of a local probe. Bubble velocities and shapes are strongly affected in the moment if it hits the sensor. For these reasons the availability of non-intrusive techniques becomes important. In the case of opaque liquids the application of acoustic or ultrasonic sensors offers a possibility to get information about the flow structure and bubble quantities. We used ultrasound Doppler velocimetry (UDV) to perform simultaneous measurements of bubble and liquid velocity. Recently, first measurements by means of UDV in bubbly flows have already been published (Suzuki et al., 2000; Wang et al., 2003), however, a number of questions with respect to the capabilities and limitations of UDV application in two-phase flows remain. Additional preparatory work has been performed to show the capability of the UDV technique to be applied for local measurements in bubbly flows (Zhang et al., 2004; Eckert et al., 2003) and especially in liquid metals (Eckert and Gerbeth, 2002; Cramer et al., 2004). In these studies the UDV technique has been shown to be suitable for velocity measurements in liquid metal two-phase flows.

The structure of the paper is arranged as follows: at first we briefly describe the experimental set-up and the measuring technique in Section 2. Section 3 contains our experimental results with respect to measurements in the liquid metal and water without magnetic field in Section 3.1 and the case of an applied magnetic field in Section 3.2, respectively. Section 3.3 is especially devoted to the alterations of the bubble wake caused by the magnetic field application.

2. Experimental set-up

The experiments were performed within an open, cylindrical container made from Perspex with a diameter $D = 100$ mm. The cylinder was filled up to a height $H = 220$ mm with the ternary alloy GaInSn as working fluid. The melting point of the eutectic composition is about 10 °C allowing measurements at room temperature. As shown in Fig. 1 the GaInSn column is positioned concentrically inside a Helmholtz configuration of two water-cooled copper coils with a vertical separa-

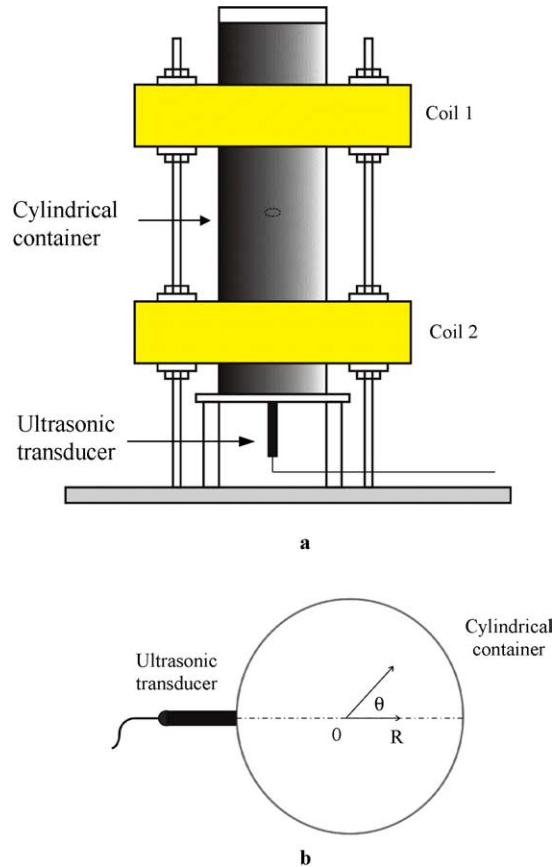


Fig. 1. Sketch of the experimental arrangement. (a) Configuration for measurements of the vertical velocity along the container axis and (b) configuration for measurements of the radial velocity.

tion of 150 mm and an inner diameter of 210 mm. This configuration provides a homogeneous DC longitudinal magnetic field over the fluid volume. The coils were supplied with a DC electric current up to 1600 A corresponding to a maximum field strength of 0.3 T. For reason of comparison measurements were also performed with water using the same experimental configuration.

Several nozzles made from stainless steel with inner diameters between 0.3 and 5 mm were used to inject argon bubbles into the bulk of the liquid. The nozzle outlet was positioned in the mid-point of the cylindrical cross-section 10 mm above the cylinder bottom. The gas flow rate was controlled using a mass flow controller (MKS 1359C, MKS Instruments). The flow rate was kept extremely low in the range between 0.002 and 0.02 cm³/s in order to guarantee a single bubble regime. The resulting intervals between two consecutive bubbles were between 5 and 15 s. The UDV measurements showed that the wake of a bubble was totally decayed within this time. Therefore, an influence on the bubble motion caused by the preceding bubble can be considered as negligible.

The DOP2000 velocimeter (model 2125, Signal Processing SA) with a standard 4 MHz transducer (TR0405LS) was used to carry out the velocity measurements. The measuring principle

of UDV uses the pulsed echo technique. Ultrasound pulses of few cycles are emitted from the transducer along the measuring line into the fluid. The method requires the occurrence of small particles moving with the flow and reflecting the ultrasound. By sampling the incoming echoes at the same time relative to the pulse emission the position shift of the particles can be measured. The knowledge of the sound velocity of the liquid allows to calculate the particle position from the time delay between the emitted pulse and the corresponding echo. In this way the UDV technique delivers an instantaneous profile of the velocity measured along the ultrasonic beam. For a more detailed description of the measuring principle we refer to Takeda (1991). The spatial resolution of the measurements is essentially controlled by the sound velocity of the liquid, the frequency of the ultrasonic bursts, the number of cycles of one burst and the size of the piezoelectric element. The measuring volume can be considered as a series of discs lined up concentrically along the measuring line. Because of the divergence of the ultrasonic beam the size of the measuring volume in lateral direction increases with the distance from the transducer. With the TR0405LS transducer used in GaInSn we achieved spatial resolutions of about 0.7 mm in axial and 10.5 mm in lateral direction in a distance of 100 mm ahead of the transducer, respectively. The measurements were carried out with a sampling frequency of 51.5 Hz. The velocity resolution was about 2 mm/s. The ultrasonic transducer was installed at the bottom wall outside of the cylinder directly behind the nozzle for the measurements of the vertical bubble and liquid velocity component. Here, the ultrasonic beam was directed vertically along the bubble path. The radial component of the liquid velocity was determined installing the transducer at the cylinder side wall. Using the UDV technique we are able to determine simultaneously the bubble and the liquid velocity. Because of the large difference in the acoustic impedance between the liquid and the gas phase the gas/liquid interface can be considered as ideal reflector for the ultrasound wave. Strictly speaking, the measured peak velocity which is taken as bubble velocity represents the vertical velocity component of the rear interface of the bubble being facing the ultrasonic transducer. The frequency of the bubble release was also evaluated. Knowing the gas flow rate which has been kept constant by the gas flow controller the equivalent bubble diameter can be calculated. The experimental arrangement of one ultrasonic transducer does not allow a measurement of the bubble shape or a tracking of the bubble path. The use of multi-sensor arrangements is currently under consideration, but has not been realized within the work presented here.

3. Results and discussion

3.1. Bubble motion in GaInSn without magnetic field

The bubble properties rising in a liquid are mainly determined by the following non-dimensional parameters:

$$\text{Reynolds number } Re = \frac{\rho_l u_T d_e}{\mu_l} \quad (1)$$

$$\text{Eötvös number } Eo = \frac{\Delta \rho g d_e^2}{\sigma} \quad (2)$$

$$\text{Morton number } Mo = \frac{\mu_1^4 \Delta \rho g}{\rho_1^2 \sigma^3} \quad (3)$$

$$\text{Weber number } We = \frac{\rho_1 u_T^2 d_e}{\sigma} \quad (4)$$

The symbols ρ , μ and σ stand for the material properties density, dynamic viscosity and surface tension. The subscript '1' denotes the liquid phase. The Reynolds number Re is based on the terminal bubble velocity u_T . Essential material properties of GaInSn and the range of non-dimensional parameters covered by our experiments are shown in Table 1. For comparison this table also contains the corresponding values for water. The equivalent bubble diameter d_e was estimated taking into account the injected gas volume V during a distinct time period and the number of bubbles n generated in the same interval according to the following equation:

$$d_e = \left(\frac{V}{n} \cdot \frac{6}{\pi} \right)^{\frac{1}{3}} \quad (5)$$

The used experimental configuration did not allow the determination of the bubble shape directly. For this reason, we use a relation given by Wellek et al. (1966) for a rough estimation. The mean aspect ratio \bar{E} of a single gas bubble rising in large fluid containers can be described as a function of the Eötvös number:

$$\bar{E} = \frac{1}{1 + 0.163 \cdot Eo^{0.757}} \quad Eo < 40, \quad Mo \leq 10^{-6} \quad (6)$$

The Eötvös number and therefore the aspect ratio \bar{E} are determined by the ratio ρ/σ which differs only by a factor of 1.14 between water and GaInSn. Therefore, we can expect basically to obtain comparable bubble shapes in GaInSn like in water. Depending on the inner diameter of the nozzle as well as on the adjusted gas flow rate in our experiments we generated gas bubbles with equivalent diameters between 4.5 and 8.5 mm. According to Eq. (6) we obtain a bubble aspect ratio between 0.76 and 0.55, respectively. Thus, we assume an oblate bubble shape being almost ellipsoidal and time-dependent. If we extrapolate the known flow regime maps (Clift et al., 1978) for our experimental parameter we have to expect the shape of the rising gas bubbles to be wobbling. The effect of contamination of the bubble surface by impurities cannot be quantified in the present

Table 1

Physical properties of the working liquids, and typical values of non-dimensional parameters at a temperature of 20 °C (calculated for the equivalent bubble diameter $d_e = 5$ mm)

	Water	GaInSn
Density ρ (kg/m ³)	998	6361
Dynamic viscosity μ (kg/m s)	9.8×10^{-4}	2.2×10^{-3}
Surface tension σ (N/m)	0.073	0.533
Electrical conductivity σ_{el} ($\Omega^{-1} \text{ m}^{-1}$)	$\approx 10^{-1}$	3.27×10^6
Morton number Mo	2.3×10^{-11}	2.4×10^{-13}
Eötvös number Eo	3.3	2.9
Reynolds number Re	1360	3000–5000
Weber number We	4.7	2.8

experiment. Generally, it causes a tendency towards an immobilization of the interface and makes the bubble stiffer.

Fig. 2 shows a typical example for the measured vertical component of the bubble velocity along the height of the liquid column. After detachment from the nozzle the bubble experienced a short period of acceleration, then the bubble velocity starts to oscillate. In transparent fluids like air–water or nitrogen–fluoroinert systems analogous phenomena were also found numerically and experimentally by other authors (Marco et al., 2003) and related to zigzag or spiral bubble motion. In the region between 100 and 200 mm the averaged value of the bubble velocity becomes almost constant and the velocity oscillation appears to be regular. Measuring quantities as the bubble terminal velocity u_T and the oscillation frequency were determined in this region. For the analysis of the motion we followed the procedure proposed by Ellingsen and Risso (2001) to fit the periodic velocity curve with a sine function (see also Fig. 2) in the form

$$u(z) = u_T + A \cdot \sin\left(\pi \frac{z - z_i}{\lambda}\right) \quad (7)$$

where A is the oscillation amplitude; z the current vertical position, z_i the initial position, and λ the wavelength. Values of u_T and λ were obtained performing a least-square fitting of the experimental results. Ensemble averages of 20 bubbles have been used to minimise the statistical error of the measurement.

The measured terminal velocities are presented in Fig. 3 vs. the equivalent bubble diameter. The data are compared with corresponding UDV measurements in tap water, experimental results published by Mori et al. (1977) for mercury and the theoretical relation given by Mendelson (1967):

$$u_T = \sqrt{\frac{2\sigma}{\rho_l d_e} + \frac{g d_e}{2}} \quad (8)$$

The experimental data obtained from the measurements in tap water and mercury match the Mendelson equation well, whereas a deviation has to be noted in the case of GaInSn. This result

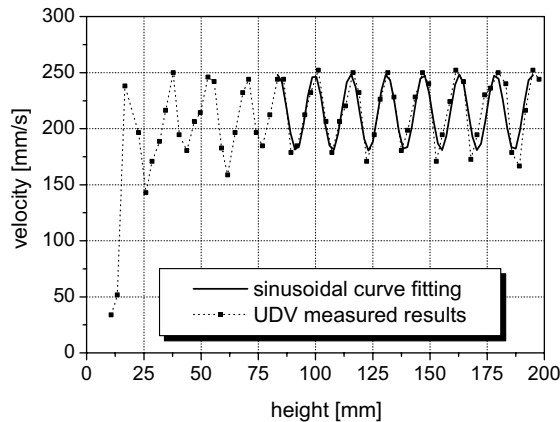


Fig. 2. Typical example of the bubble vertical velocity measured along the height of the fluid container ($d_e = 4.6$ mm, $B = 0$).

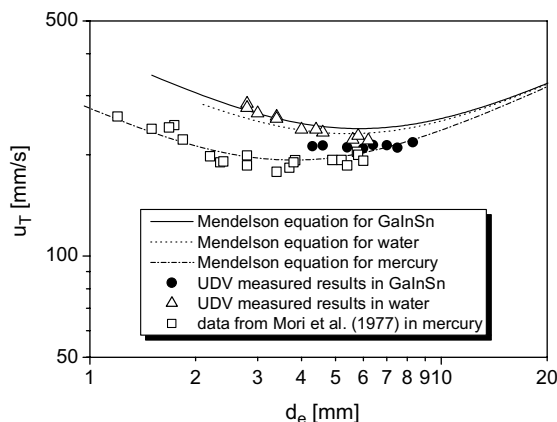


Fig. 3. Terminal bubble velocity vs. equivalent bubble diameter in various liquids.

is seemingly attributed to the role of impurities in the melt. In contrast to the noble metal mercury a distinct oxidation of the liquid GaInSn alloy cannot be avoided with reasonable effort in our experiment. On one hand the Mendelson curve should proceed closer to the measured values if one considers a lower surface tension in Eq. (8) as suggested by our practical experiences that the occurrence of oxides diminishes the surface tension significantly (see also Szekely, 1979). Moreover, a considerable increase of the drag arises from a more rigid bubble interface which slows down the flow at the rear of the bubble (Magnaudet and Eames, 2000; Cuenot et al., 1997).

The same tendency can also be observed in Fig. 4 where the drag coefficient C_D was drawn as a function of the Reynolds number Re . These results are based on the data of the terminal velocity already presented in Fig. 3 using the following equation:

$$C_D = \frac{4}{3} \frac{\Delta \rho d_e g}{u_T^2 \rho_1} \quad (9)$$

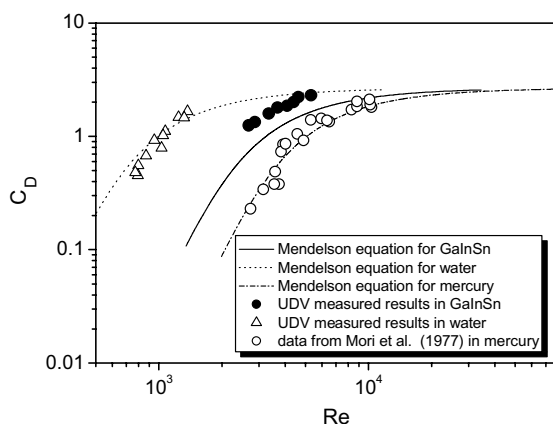


Fig. 4. Bubble drag coefficient vs. bubble Reynolds number in various liquids.

As shown in Fig. 4, the drag coefficient increases with increasing Re . It indicates that bubbles rise along a non-rectilinear trajectory and flow separations probably occur behind them (Saffman, 1956). We can also notice that in the parameter range considered here the characteristic drag coefficient for spherical-cap bubbles (Clift et al., 1978) is not reached.

From the wavelength λ determined from the experimental results using Eq. (7) the oscillation frequency f of the vertical bubble velocity was deduced as $f = u_T/\lambda$. The obtained results displayed in Fig. 5 show an almost monotonic decrease with increasing equivalent bubble diameter. Our data are shown together with results published by Zun and Groselj (1996) for air bubbles in water. They measured frequencies of the bubble path in the horizontal cross-section and they too found the oscillation frequency to decrease with increasing bubble size for bubbles with an equivalent diameter larger than 3 mm. It is already known from Ellingsen and Risso (2001) and Fan and Tsushiya (1990) that the oscillation frequency of the bubble motion in the vertical plane is about twice that in the horizontal one which is also confirmed by the comparison presented in Fig. 5. To facilitate the comparison, we plotted twice the frequency measured by Zun and Groselj (1996) in the same figure as well. However, one has to note that the measurements shown in Fig. 5 were carried out in water and GaInSn with significantly different ranges of the Morton and Reynolds numbers.

The oscillation of the terminal rising velocity of the bubbles was also analysed in terms of the Strouhal number $St = f \cdot d_e/u_T$. In Fig. 6 the Strouhal number St is drawn as a function of the Reynolds number Re . Our results are compared with data published by Lindt (1972), who studied the $St-Re$ relationship for air bubbles in tap water. In his work the Strouhal number was determined by counting the vortices shedding from the bubble on stroboscopic flash photographs. It turned out that the Strouhal number increases with increasing Reynolds number for $Re < 3000$ whereas St is almost constant at higher Re . Our measurements show a fairly good agreement with Lindt's data.

The results of the UDV measurements presented in this section provide essential information about the bubble motion in the liquid metal without magnetic field. At the experimental condi-

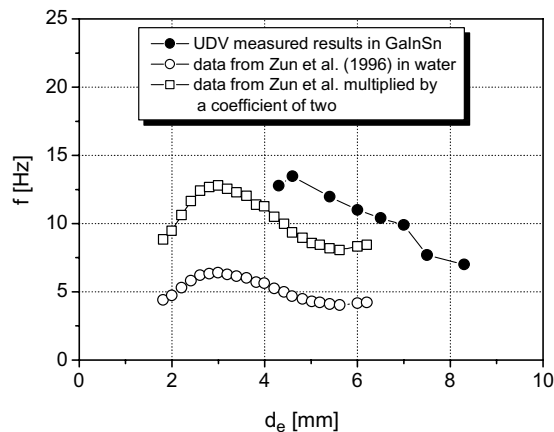


Fig. 5. Frequency of oscillations of vertical bubble velocity vs. equivalent bubble diameter.

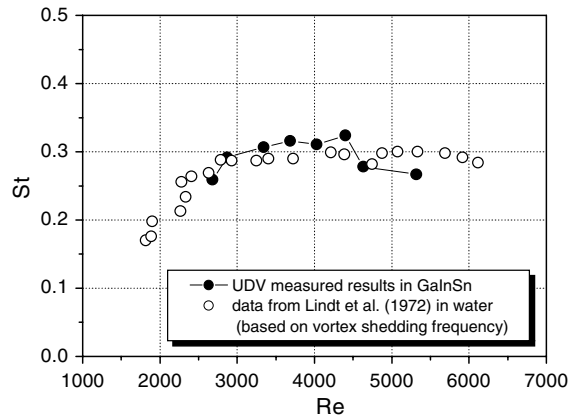


Fig. 6. Bubble Strouhal number vs. Reynolds number.

tions considered in the present paper we can assume that we have almost ellipsoidal bubbles with an oscillating interface and that they rise on a zigzag path.

3.2. Bubble motion affected by a DC magnetic field

There is plenty of information available on the nature of electrically conducting liquids flowing under the influence of a steady magnetic field. The behaviour of vortex structures in a static magnetic field has been studied in detail, for instance, by Davidson (1995, 2001) or Sreenivasan and Alboussiere (2002). The main effect of a DC magnetic field applied onto the turbulent motion of an electrically conducting fluid consists in an anisotropic suppression of the mean velocity and the turbulent fluctuations, whereas vortices with axes being aligned with the magnetic field direction are not affected by the electromagnetic damping. The process can be described as the propagation of momentum along the magnetic field lines. As a result, the flow field becomes anisotropic in the sense that it will be independent on the coordinate parallel to the field. In this section we study the consequences of this magnetic field action for the behaviour of a rising gas bubble.

Fig. 7 compares the vertical bubble velocity obtained at an applied field strength of 0.17 T with corresponding data for the case without magnetic field. The curves result from an ensemble average using 10 bubbles. The bubble motion inside the magnetic field shows a slightly higher mean value of the terminal velocity, and the shape and amplitude of the velocity oscillations appear more regular.

For a detailed discussion of the magnetic field influence on the bubble behaviour we introduce a further non-dimensional parameter, the magnetic interaction parameter N , describing the ratio between electromagnetic and inertial forces

$$N = \frac{\sigma_{el} B^2 d_e}{\rho_l u_T} \quad (10)$$

where σ_{el} stands for the electrical conductivity of the liquid. The dependence of the drag coefficient C_D on the interaction parameter N is shown in Fig. 8 for several values of the Eötvös number Eu .

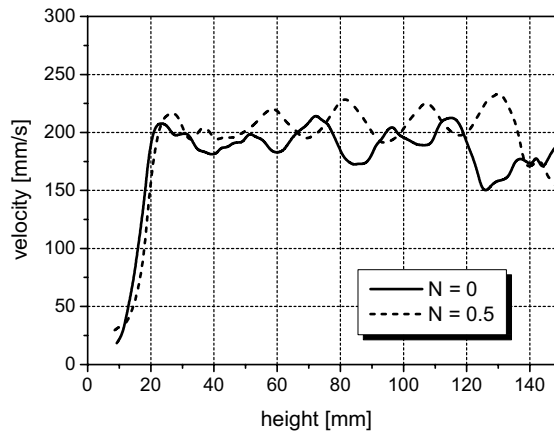


Fig. 7. Typical example demonstrating the influence of the longitudinal DC magnetic field on the bubble velocity.

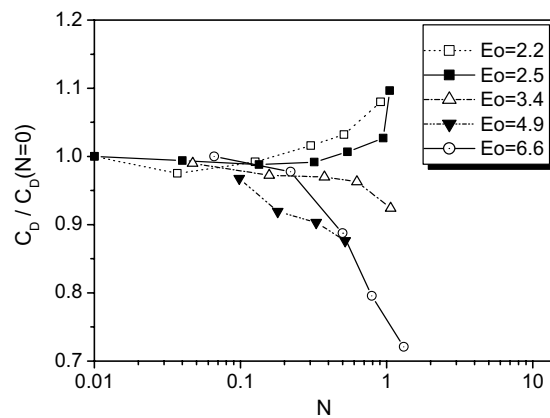


Fig. 8. Drag coefficient vs. magnetic interaction parameter.

Here, the presented data were normalised with the corresponding drag coefficient obtained without magnetic field $C_D(N=0)$. In the investigated parameter range $N < 2$ two different tendencies become obvious. For small bubbles ($Eo \leq 2.5$) the application of the magnetic field finally leads to an increase of the drag coefficient. On the other hand, larger bubbles ($Eo \geq 3.4$) experience a reduction of the drag coefficient.

The only previous experimental work dealing with a flow around a solid sphere aligned with the direction of a DC magnetic field were performed by Maxworthy (1962, 1968) and Yonas (1967). We are not aware of adequate studies with respect to single gas bubbles. Yonas and Maxworthy measured the drag coefficient of rigid spheres at large interaction parameters $0 < N < 80$ and Reynolds numbers between $10^4 < Re < 25 \times 10^4$. In contradiction to our results they reported a monotonic increase of the drag with growing magnetic field strength. Compared with the case of the solid sphere the bubble motion has to be considered as a more complex phenomenon because

the bubble shape and trajectory can undergo distinct modifications. Mori et al. (1977) investigated single N_2 bubbles rising in a mercury tank exposed to a transverse magnetic field. For a bubble diameter of about 2.3 mm, Mori et al. found the rise angle between the bubble velocity and the vertical reference line to decrease with increasing magnetic field strength B . The bubbles rise vertically if B reaches a value of about 1.5 T. Consequently, C_D decreases with increasing magnetic field intensity. On the other hand, for larger bubbles taking the shape of spherical cap bubbles the same $C_D(N)$ tendency was observed as known for a solid sphere. The drag coefficient displayed in Fig. 8 of the present study was calculated from Eq. (9) using the measured vertical component of the bubble velocity as terminal velocity u_T . In the parameter range covered by our experiments the bubbles do not rise along a rectilinear trajectory. Oscillations of the vertical bubble velocity indicate the occurrence of horizontal velocity components. The application of the longitudinal magnetic field suppresses the liquid motion in the direction perpendicular to the magnetic field lines, thus diminishing also the lateral components of the bubble velocity. As displayed in Fig. 9 the amplitude of the vertical velocity oscillations decreases with increasing magnetic interaction parameter N . In parallel we measure a higher vertical velocity of the rising bubble. Consequently, the reduction of the drag coefficient may result from a modification of the bubble path caused by the magnetic field.

The electromagnetic damping of the horizontal components of the liquid velocity is demonstrated in Fig. 10 where velocity profiles measured along the diameter of the cylindrical vessel at a height of 100 mm are presented. The profiles were recorded 0.4 s after the bubble passage at this position. If a magnetic field of 0.17 T is applied the amplitude of radial velocity in the wake is observed to be up to 5 times lower as in the case without magnetic field.

Such an effect as observed in the present paper for a single bubble was also found for bubble clouds in a vertical channel flow injected by an orifice positioned in the channel center of the cross-section (Eckert et al., 2000a). Here, the turbulent bubble dispersion was significantly reduced by the magnetic field resulting in a narrow peak of void distribution above the injector position.

Fig. 11 contains the dependence of the Strouhal number St calculated from the bubble velocity oscillations on the magnetic interaction parameter N . It becomes obvious that the magnetic field

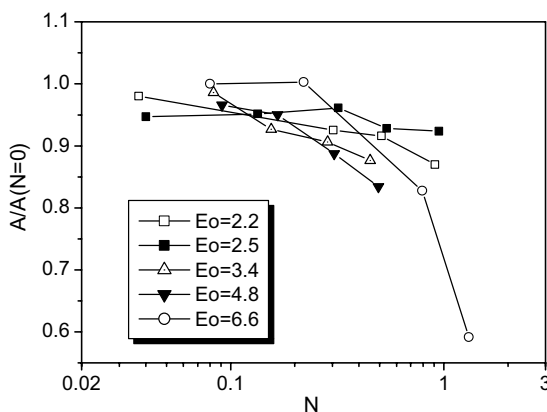


Fig. 9. Velocity oscillation amplitude vs. interaction number.

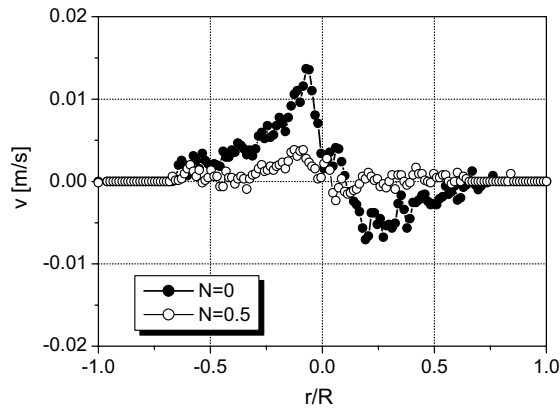


Fig. 10. Snapshot of the radial velocity component with and without applied longitudinal DC magnetic field after the passage of a bubble ($t = 0.4$ s, $t/T = 3.1$).

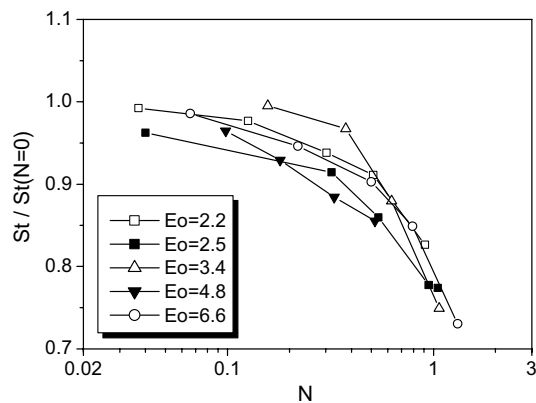


Fig. 11. Bubble Strouhal number vs. magnetic interaction parameter.

considerably influences the structures in the bubble wake. The wave length λ of the measured velocity oscillations becomes larger with increasing N corresponding to a reduction of St as shown in Fig. 11. The same tendency was found from measurements in a cylinder wake if the direction of magnetic field is chosen parallel to the mean flow (Lahjomri et al., 1993). The authors explain the reduced generation of vorticity by the Joule effect. The magnetic field delays the growth of eddies that form on the cylinder surface, and, therefore, their detachment by the external flow. As a consequence, the shedding frequency of vortices is lowered.

Vertical velocity measurements along the cylinder axis also reveal the magnetic field influence on the bubble wake. Snapshots from these measurements shown in Fig. 12 were acquired at those moments when the bubble was detected at vertical positions of 130 mm and 170 mm, respectively. In the case without magnetic field the vortex structure of the wake can clearly be recognized in the signal. One may conclude from Fig. 12 that in the case without magnetic field the wake is not fully developed yet, before the bubble has reached a height of approximately 70 mm, because distinct oscillations of the vertical liquid velocity cannot be observed in this region. The vertical liquid

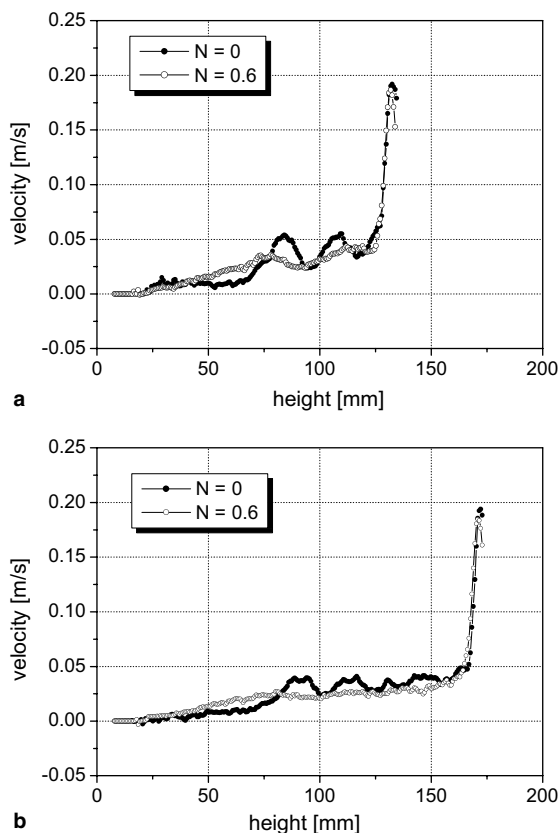


Fig. 12. Snapshots of the vertical velocity in the bubble wake when the bubble has reached a vertical height of 130 mm (a) and 170 mm (b), respectively.

velocity behind the bubble generally becomes more uniform if the magnetic field is turned on, in other words the velocity gradient along the field lines is significantly reduced. Besides the damping of the velocity in the wake region, an elongation of the wake structure in vertical direction due to the anisotropy of the magnetic field influence can be observed. This fact is coupled with longer decay times of the bubble induced velocity in the far wake region. The temporal development of the bubble induced velocity on the centerline of the fluid cylinder at heights of 66 mm and 100 mm, respectively, is drawn in Fig. 13. Here, the velocity was normalized with the terminal bubble velocity u_T , and the time axis was normalized with the mean period of the detected velocity oscillations $T = \lambda/u_T$ of the rising bubble. For both vertical positions presented in Fig. 13 the liquid velocity just behind the bubble appears smaller with magnetic field, and the amplitude decays more slowly. It is worth to recall, that the UDV technique provides a spatial average of the velocity inside the measuring volume which is about 1 mm along the ultrasonic beam and 10 mm in lateral direction. Thus, smaller velocity structures with strong gradients occurring certainly in the region behind the bubble cannot be resolved in detail.

It is known that the flow structure is distinctly affected by a DC magnetic field if the magnetic interaction parameter N exceeds the value of 1. The electromagnetic dissipation term reveals a

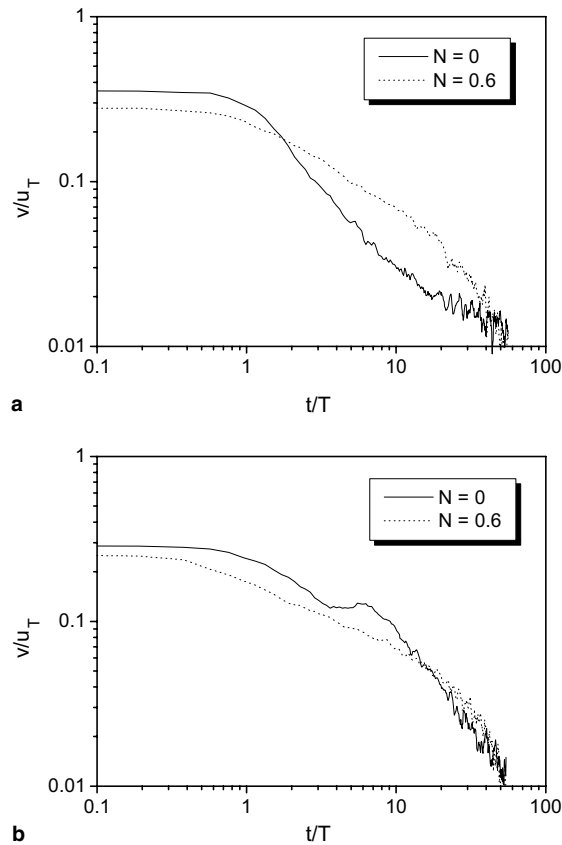


Fig. 13. Decay of the vertical liquid velocity induced by a 7 mm bubble with and without applied magnetic field ($t = 0$, if the gas–liquid interface passes the measuring position). At the height of 66 mm (a) and 100 mm (b).

strong anisotropy. As shown by Sommeria and Moreau (1982) vortices are weakly damped if their axes are parallel with respect to the magnetic field lines. Turbulent kinetic energy can be transferred from flow structures perpendicular to the magnetic field direction towards the parallel velocity component. This spreading of momentum along the magnetic field lines is a well-known phenomenon in the context of MHD turbulence leading to an elongation of the flow parallel to the magnetic field (Davidson, 1995). Note that our experiments have not been carried out in the range of $N \gg 1$ where such an elongation of vortices parallel to the magnetic field direction occurs, although an expansion of the bubble wake in vertical direction can be observed in Fig. 12. Knowledge about the wake behind bubbles rising in transparent liquids was obtained from visualization techniques by several authors and reviewed by Ellingsen and Risso (2001). Lunde and Perkins (1997) found the wake of bubbles rising along a helical trajectory consists of two attached vortex filaments whereas hairpin-like vortex structures were associated with bubbles showing a zigzag or rocking motion. Such observations were confirmed by Brücker (1999) relating the zigzag bubble path to the alternate shedding of oppositely oriented hairpin-like vortices. How should such a vortex structure be affected by a longitudinal magnetic field? The axes of the legs

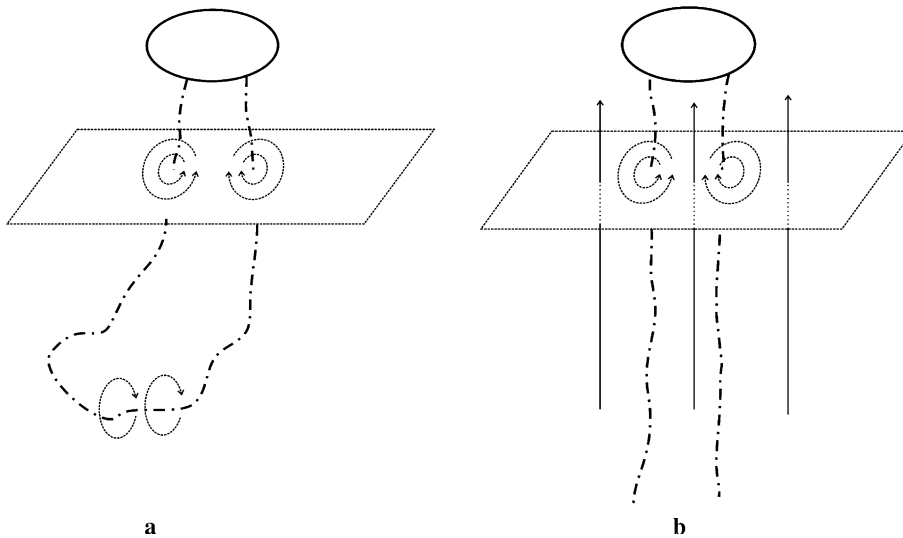


Fig. 14. Sketch of the bubble wake structure in a longitudinal DC magnetic field. (a) Without magnetic field and (b) within a longitudinal DC magnetic field.

of a hairpin vortex are almost aligned with the direction of the vertically applied magnetic field. According to the knowledge about MHD turbulence we expect only a weak damping for such vortices, but a straightening and more strict alignment with the field lines should occur as sketched in Fig. 14. On the other hand, the head of the hairpin vortex should fully be governed by the Joule dissipation resulting in an efficient damping. According to these considerations it can be observed in Fig. 12 that the oscillations of the liquid vertical velocity obviously disappear if the magnetic field is applied.

4. Conclusions

The non-intrusive UDV measuring technique has been used to study the motion of single bubbles rising in a liquid metal column. The consequence of an application of a longitudinal magnetic field on the bubble and liquid velocity was investigated. The UDV technique offers a possibility to measure in opaque liquids both bubble and liquid velocities simultaneously. The method delivers instantaneous velocity profiles along the path of the ultrasonic beam allowing an analysis of the spatial flow structure.

Measurements performed in GaInSn without magnetic field were analyzed in terms of the terminal velocity, the drag coefficient, the oscillation frequency of the bubble velocity and the Strouhal number. Taking into account the contamination of the metallic alloy mainly caused by oxidation our results agree well with the well-known Mendelson equation and existing experimental data obtained in water and mercury, respectively.

The interest of the present paper was focussed on the impact of an external, longitudinal magnetic field on the bubble motion. The measurements reveal a distinct effect of the magnetic field on

the bubble velocity as well as the bubble wake. The magnetic field application leads to a mitigation of the horizontal components of the bubble velocity resulting in a more rectilinear bubble path. As a consequence a reduction of the drag coefficient with increasing magnetic field strength was observed for bubble diameters larger than 5.4 mm. On the other hand, small bubbles ($d_e \leq 4.6$ mm) show qualitatively the same behavior as found in studies of solid spheres, e.g. raising the magnetic interaction parameter increases the drag coefficient. The Strouhal number derived from the oscillations of the bubble velocity was found to monotonically decrease with increasing magnetic interaction parameter. Because the bubble is electrically non-conducting the magnetic field effect on the bubble motion should take place indirectly by changes of the liquid flow structure. The measurements show that both vertical and radial velocity components of the liquid were modified by the exposition of the magnetic field. As a result of the interaction between magnetic field and liquid flow electric currents were induced inside the liquid causing a damping of the flow by Joule dissipation. However, a characteristic feature of the electromagnetic dissipation is the anisotropy. Vortices such as the ‘legs’ of hairpin-like structures in the bubble whose axis are almost aligned with the magnetic field direction should be weakly affected whereas the non-horizontal vortices will be fully governed by Joule dissipation. As demonstrated in the experiments the magnetic field suppresses liquid velocity oscillations in the bubble wake. In this way the flow structure is kept to be almost two-dimensional, that means a transition from the two attached vortex filaments in the bubble wake towards the three-dimensional hairpin-like structures is impeded. The corresponding decay rate of the liquid velocity in the wake was shown to be smaller as compared to the case without magnetic field application.

Because of the lack of suitable experimental capabilities to determine the bubble shape, until now the interpretation of the observed tendencies regarding the drag coefficient or the vortex shedding does not consider any possible influence arising from the bubble deformation, which is probably also modified by the magnetic field application. Measurements of the bubble shape are possible using a three-point electrical resistivity probe (Mori et al., 1977). However, the application of such an invasive sensor may disturb the bubble behavior significantly. One way to handle this problem might be to expose gas bubbles in transparent electrolytes to strong magnetic fields of the order of 10 T (Furuhashi et al., 2004). In further studies with liquid metals it is foreseen to use non-invasive techniques such as the X-ray radiography for this purpose.

The proposed physical mechanism of the reorganization of the bubble wake resulting from the application of the magnetic field appears plausible with respect to the existing knowledge about MHD turbulence, but cannot explain all observed trends accurately. Therefore, a comprehensive explanation of the bubble motion under the influence of a DC magnetic field needs further investigations. In a next step we will study the single bubble motion in a transverse magnetic field. Moreover, to broaden the informational content of the measurements the application of multiple sensor arrangements allowing a two-dimensional flow mapping is planned in future.

Acknowledgments

The research is supported by the Deutsche Forschungsgemeinschaft (DFG) in form of the SFB 609 “Electromagnetic Flow Control in Metallurgy, Crystal Growth and Electrochemistry”. This support is gratefully acknowledged by the authors. Furthermore, the authors wish to express their

thanks to J. Hueller and T. Gundrum for their valuable support in the chemical preparation of the metallic alloy and the set-up of the electric equipment.

References

- Andreini, R.J., Foster, J.S., Callen, R.W., 1977. Characterization of gas bubbles injected into molten metals under laminar flow conditions. *Met. Trans.* 8B, 625–631.
- Brücker, C., 1999. Structure and dynamics of the wake of bubbles and its relevance for bubble interaction. *Phys. Fluids* 11, 1781–1796.
- Cartellier, A., Barrau, E., 1998. Monofiber optical probes for gas detection and gas velocity measurements: conical probes. *Int. J. Multiphase Flow* 24, 1265–1294.
- Clift, R., Grace, J., Weber, M., 1978. *Bubbles, drop and particles*. Academic Press, New York.
- Cramer, A., Zhang, C., Eckert, S., 2004. Local structures in liquid metals measured by ultrasonic Doppler velocimetry. *Flow Meas. Instrum.* 15, 145–153.
- Cuenot, B., Magnaudet, J., Spennato, B., 1997. The effects of slightly soluble surfactants on the flow around a spherical bubble. *J. Fluid Mech.* 339, 25–53.
- Davidson, P.A., 1995. Magnetic damping of jets and vortices. *J. Fluid Mech.* 299, 153–186.
- Davidson, P.A., 2001. *An introduction to magnetohydrodynamics*. Cambridge University Press, Cambridge.
- Eckert, S., Gerbeth, G., 2002. Velocity measurements in liquid sodium by means of ultrasound Doppler velocimetry. *Exp. Fluids* 32, 542–546.
- Eckert, S., Gerbeth, G., Melnikov, V.I., 2003. Velocity measurements at high temperatures by ultrasound Doppler velocimetry using an acoustic wave guide. *Exp. Fluids* 35, 381–388.
- Eckert, S., Gerbeth, G., Lielausis, O., 2000a. The behavior of gas bubbles in a turbulent liquid metal magnetohydrodynamic flow. Part I: Dispersion in quasi-two-dimensional magnetohydrodynamic turbulence. *Int. J. Multiphase Flow* 26, 45–66.
- Eckert, S., Gerbeth, G., Lielausis, O., 2000b. The behavior of gas bubbles in a turbulent liquid metal magnetohydrodynamic flow. Part II: Magnetic field influence on the slip ratio. *Int. J. Multiphase Flow* 26, 67–82.
- Ellingsen, K., Risso, F., 2001. On the rise of an ellipsoidal bubble in water: oscillatory paths and liquid-induced velocity. *J. Fluid Mech.* 440, 235–268.
- Fan, L.S., Tsushiya, K., 1990. *Bubble wake dynamics in liquids and liquid–solid suspensions*. Butterworth-Heinemann, Stoneham.
- Furuhashi, I., Iwai, K., Asai, S., 2004. Simulated observation of the bubble motion in a continuous casting with an electromagnetic brake. *CAMP-ISIJ* 17, 111.
- Iguchi, M., Nakatani, T., Kawabata, H., 1997. Development of a multineedle electroresistivity probe for measuring bubble characteristics in molten metal baths. *Met. Mat. Trans.* 28B, 409–416.
- Lahjomri, J., Caperan, P., Alemany, A., 1993. The cylinder wake in a magnetic field aligned with the velocity. *J. Fluid Mech.* 253, 421–448.
- Lindt, L.T., 1972. On the periodic nature of the drag on a rising bubble. *Chem. Eng. Sci.* 57, 1775–1781.
- Lunde, K., Perkins, R.J., 1997. Observation on wakes behind spheroidal bubbles and particles. No. FEDSM97-3530
- Magnaudet, J., Eames, I., 2000. The motion of high-Reynolds-number bubbles in inhomogeneous flows. *Ann. Rev. Fluid Mech.* 32, 659–708.
- Marco, P., Grassi, W., Memoli, G., 2003. Experimental study on rising velocity of nitrogen bubbles in FC-72. *Int. J. Thermal Sci.* 42, 435–446.
- Maxworthy, T., 1962. Measurements of drag and wake structure in magneto-fluid dynamic flow about a sphere. *Proceedings of the 1962 Heat Transfer and Fluid Mechanics Institute*, 197–205
- Maxworthy, T., 1968. Experimental studies in magneto-fluid dynamics: pressure distribution measurements around a sphere. *J. Fluid Mech.* 31, 801–814.
- Mendelson, H.D., 1967. The prediction of bubble terminal velocity from wave theory. *AIChE J.* 13, 250–253.
- Mori, Y., Hijikata, K., Kuriyama, K., 1977. Experimental study of bubble motion in mercury with and without a magnetic field. *J. Heat Transfer (Trans. ASME)* 99, 404–410.

- Saffman, P.G., 1956. On the rise of small air bubbles in water. *J. Fluid Mech.* 1, 249–275.
- Schwerdtfeger, K., 1968. Velocity of rise of argon bubbles in mercury. *Chem. Eng. Sci.* 23, 937–938.
- Sommeria, J., Moreau, R., 1982. Why, how, and when, MHD turbulence becomes two-dimensional. *J. Fluid Mech.* 118, 507–518.
- Sreenivasan, B., Alboussiere, T., 2002. Experimental study of a vortex in magnetic field. *J. Fluid Mech.* 464, 287–309.
- Suzuki, Y., Aritomi, M., Kikura, H., 2000. Measurement of the flow around bubbles using the ultrasonic velocity profile monitor. *Bull. Res. Lab. Nucl. Reactors (Tokyo Institute of Technology)* 3, 93–99.
- Szekely, J., 1979. *Fluid flow phenomena in metals processing*. Academic Press, New York.
- Takeda, Y., 1991. Development of an ultrasound velocity profile monitor. *Nucl. Eng. Des.* 126, 277–284.
- Toral, H., 1981. A study of the hot-wire anemometer for measuring void fraction in two-phase flow. *J. Phys. E Sci. Instrum.* 14, 822–827.
- Wang, T., Wang, J., Ren, F., Jin, Y., 2003. Application of Doppler ultrasound velocimetry in multiphase flow. *Chem. Eng. J.* 92, 111–122.
- Wellek, R.M., Agrawal, A.K., Skelland, A.H.P., 1966. Shapes of liquid drops in liquid media. *AIChE* 12, 854–862.
- de Vries, A.W.G., Biesheuvel, A., van Wijngaarden, L., 2002. Notes on the path and wake of a gas bubble rising in pure water. *Int. J. Multiphase Flow* 28, 1823–1835.
- Yonas, G., 1967. Measurements of drag in a conducting fluid with an aligned field and large interaction number. *J. Fluid Mech.* 30, 817–823.
- Zhang, C., Eckert, S., Gerbeth, G., 2004. Gas and liquid velocity measurements in bubble chain driven two-phase flow by means of UDV and LDA. In: *Proceedings of the 5th International Conference on Multiphase Flow, Yokohama, Japan, No. ICMF04-260*
- Zun, I., Groselj, J., 1996. The structure of bubble non-equilibrium movement in free-rise and agitated-rise conditions. *Nucl. Eng. Des.* 163, 99–115.